Fluid Phase Equilibria 557 (2022) 113420

Contents lists available at ScienceDirect

Fluid Phase Equilibria

journal homepage: www.elsevier.com/locate/fluid

Optimal experimental design of physical property measurements for optimal chemical process simulations☆

Lorenz Fleitmann[a,b], Jan Pyschik[b], Ludger Wolff[b], Johannes Schilling[a,b], André Bardow[a,b,c,*]

[a] Energy and Process Systems Engineering, Department of Mechanical and Process Engineering, ETH Zurich, Tannenstrasse 3, Zurich 8092, Switzerland
[b] Institute for Technical Thermodynamics, RWTH Aachen University, Schinkelstrasse 8, Aachen 52062, Germany
[c] Institute for Energy and Climate Research - Energy Systems Engineering (IEK-10), Forschungszentrum Jülich GmbH, Wilhelm-Johnen Strasse, Jülich 52425, Germany

ARTICLE INFO

Article history:
Received 31 October 2021
Revised 17 January 2022
Accepted 12 February 2022
Available online 15 February 2022

Keywords:
Model-based experimental design
Simulation uncertainty
Parameter precision
Liquid-liquid-equilibrium
Extraction-distillation

ABSTRACT

Chemical process simulations depend on physical properties, which are usually available through property models with parameters estimated from experiments. The required experimental effort can be reduced using the method of Optimal Experimental Design (OED). OED reduces the number of experiments by minimising the expected uncertainty of the estimated parameters. In chemical engineering, however, the main purpose of an experiment is usually not to determine property parameters with minimum uncertainty but to simulate processes accurately. Therefore, this paper presents the OED of physical property measurements resulting in the most accurate process simulations: c-optimal experimental design (c-OED). c-OED aims to minimise the uncertainty of the process simulation results, which is estimated by linear uncertainty propagation from uncertain property parameters through the process model. We use c-OED to design liquid-liquid equilibrium and diffusion experiments minimising thermodynamic and economic performance metrics of three solvent-based processes. In all three case studies, the c-optimal design substantially reduces the experimental effort for the same simulation accuracy compared to state-of-the-art OED that neglects the process. Our findings are confirmed by a Monte-Carlo simulation of the designed experiments. Furthermore, we assess the limits of c-OED for highly nonlinear process models. Thus, the work shows how c-OED can successfully reduce experimental effort required for accurate process simulations by tailoring experimental designs to the process model.

1. Introduction

For the simulation and design of chemical processes, estimation of physical properties is crucial [1]. In particular, thermodynamic properties, e.g. describing phase behaviour, largely influence chemical processes [2]. Therefore, accurate simulations in chemical engineering require high-quality property data. Today, the basis for accurate property parameter estimation is still mostly experimentation [3]. The experimental data is then usually used to fit parameters in physical property models to allow for interpolation or even extrapolation in the simulations. However, experiments consume time and large amounts of materials causing high costs for estimating parameters in property models. Therefore, experimental effort should be minimised by selecting only experiments that provide the most information and thus lead to the most accurate process simulations.

Selecting optimal experiments is an important topic and has led to establishing the theory of model-based optimal experimental design (OED) [4,5]. OED identifies optimal experiments by analysing the uncertainty propagation from experimental measures to estimated property parameters through a predefined model of the experiment. So far, OED has been applied for the estimation of important thermodynamic properties in chemical engineering, such as reaction kinetics [6,7], phase equilibria [8,9], diffusion coefficients [10] or adsorption isotherms [7].

Generally, two approaches for OED can be distinguished: (1) statistical OED [5] and (2) bounded-error OED [11]. Statistical OED minimises the parameter variances considering a statistical error distribution [7]. In contrast, bounded-error OED minimises the feasible parameter set consistent with the measurement uncertainty

☆ Supporting Information available online at LINK SI.

* Corresponding author at: Energy and Process Systems Engineering, Department of Mechanical and Process Engineering, ETH Zurich, Tannenstrasse 3, 8092 Zurich, Switzerland.
E-mail address: abardow@ethz.ch (A. Bardow).

https://doi.org/10.1016/j.fluid.2022.113420
0378-3812/

Nomenclature

α	scalar measure describing the center of the tie lines
$\boldsymbol{A}$	matrix containing the sensitivities of the thermodynamic model $\boldsymbol{g}$ with respect to the experimental measurements $\boldsymbol{w}$
$\boldsymbol{B}$	matrix containing the sensitivities of the thermodynamic model $\boldsymbol{g}$ with respect to the parameters $\boldsymbol{\theta}$
$\boldsymbol{c}$	vector containing the sensitivities of the process model h with respect to the parameters $\boldsymbol{\theta}$
$\boldsymbol{F}$	Fisher-Information-Matrix
$\boldsymbol{g}$	thermodynamic model describing the experiments
h	process model result
$\boldsymbol{\kappa}$	parameters of the process model
N	number of distinct experimental settings
N_{exp}	number of experiments
Q_{min}	minimum reboiler energy demand calculated by pinch-based distillation model
σ_{w}	standard deviation of measurements
S_{min}	minimum solvent demand calculated by pinch-based extraction model
$\boldsymbol{\theta}$	thermodynamic model parameters
$\hat{\boldsymbol{\theta}}$, $\hat{\boldsymbol{\kappa}}$	initial or predefined parameters of $\boldsymbol{\theta}$ or $\boldsymbol{\kappa}$
$\boldsymbol{\Sigma}_0$	parameter variance-covariance matrix from previously performed experiments
$\boldsymbol{V}_{\text{w}}$	variance-covariance matrix of the experimental measurements $\boldsymbol{w}$
V_δ	variance-covariance matrix of the parameters δ
v_i	normalised weight of experiment i
$\boldsymbol{w}$	experimental measurement results
$\boldsymbol{\xi}$	design vector describing an experimental design
$\boldsymbol{\xi}^*$	optimal experimental design vector
$\boldsymbol{\xi}_{\text{con}}$	conventional experimental design
$\boldsymbol{\xi}_{\text{c}}^*$, $\boldsymbol{\xi}_{\text{D}}^*$	c- and D-optimal experimental design, respectively
$\boldsymbol{z}_i$	experimental settings for experiment i
ζ_{c}, ζ_{D}	c- and D-efficiency, respectively

given by upper and lower bounds on the errors [7]. As a result, bounded-error OED requires fewer assumptions on errors than statistical OED but instead needs to solve a challenging bilevel optimisation problem. For many experiments in chemical engineering problems, the measurement uncertainty is known [12] and justifies the use of statistical OED. Thus, in this work, we focus on the more popular statistical OED.

In statistical OED, the objective function is usually a scalar measure of the parameter variances representing parameter uncertainty [5]. Several well-known objective functions have been developed to determine the experimental designs leading to the most accurate parameters [5], e.g. minimising the average uncertainty of all parameters (A-optimality); minimising the uncertainty of the most uncertain parameter (E-optimality); or minimising a generalised variance of the parameters (D-optimality).

However, in chemical engineering, the primary purpose of experiments is rarely to gain knowledge of parameters themselves. Instead, chemical engineers, e.g. seek to gain thermodynamic insights, predict phase behaviours or simulate a process. Thus, the experimental design needs to reflect the model application [13]. Recently, OED methods have focused on incorporating the purpose of parameter estimation. [8] employed G-optimal experimental design that minimises the expected variance of the model predictions of the experiments of uncertainties in property parameters. In particular, [8] minimised the predicted variance of phase compositions calculated from a liquid-liquid equilibrium model instead of the property parameters of the used activity coefficient model.

Similarly, for process simulations, the impact of the property parameters on the simulation results is usually more important than the uncertainty of the property parameters. If the governing phenomena of the chemical system are known and a thermodynamic model capable to describe these phenomena is selected, the purpose of experimentation is accuracy increase of the simulation through (re-)parametrisation. However, an experimental design for the most accurate property parameters does not ensure the lowest uncertainty in process simulation. Thus, the property parameter use in a process model needs to be considered within the optimal experimental design.

For this purpose, [14] recently presented OED for experiments in a plant or mini plant using a flowsheet simulator. In their work, the optimal experimental design considers property parameter use by employing the process model already for the parameter estimation. The authors show that their method improves model discrimination and parameter estimation. However, the method requires expensive and time-consuming plant experiments instead of small lab-scale experiments.

For lab-scale experiments and bounded-error OED, Walz and coworkers accounted for property parameter use in process simulation and design [7,15]. The authors successfully show how to reduce experimental effort without changing the reliability of the process model results. However, their method requires solving a challenging bi- or trilevel optimisation problem and is currently limited to small process models.

For statistical OED and lab-scale experiments, a first approach was published by Recker et al. [16]. The authors considered the sensitivities of the process to the property parameters by heuristically scaling the A-optimality criterion and successfully optimised the experimental design to estimate reaction kinetics for a reaction-separation process. A similar approach was proposed by Lucia and Paulen [17] for robust nonlinear model predictive control. Using the sensitivities of the optimal robust economic objective value to parametric uncertainty, the authors scaled a modified E-criterion. Kaiser and Engell [18] and Kaiser et al. [19] linked OED for parameter estimation with superstructure optimisation of early process design stages [18,19]. For this purpose, the authors perform global sensitivity analysis of optimisation results towards the uncertain parameters using heuristically scaled D-optimality [18] and heuristically scaled A-optimality [19].

However, even though these heuristic approaches provide a breakthrough by combining OED and process simulation, heuristic designs likely differ from optimal designs with full consideration of the process [20]. Instead, full consideration of process information requires uncertainties of property parameters to propagate through the process model, and the uncertainties of the process model results should be used as the OED objective.

In pioneering work, the van Impe group integrated experimental design and nonlinear model predictive control [21–23]. The authors mathematically derived an economic process objective function for experimental design by weighted A-optimality. They defined the OED objective as the minimisation of the expected optimality gap of the parametric optimal control problem via second-order derivatives of the Lagrange function [21]. The approach was demonstrated successfully to tailor experimental designs for estimating reaction rate constants to control problems of bioreactors.

Similarly, for the most accurate chemical process simulations, the OED objective needs to be defined in terms of process uncertainties to capture the property parameter use in the process simulation. The idea of optimising the uncertainty of a simulation output as the objective for OED can be formulated as the so-called c-optimal experimental design (c-OED) [4]. In general, c-OED minimises a linear combination of model parameter variances as the optimisation objective [4]. A linear combination of model parameters corresponds to the linear variance propagation of these pa-

rameters through a model if the weights of the linear combination are the first-order derivatives of the model with respect to the model parameters. Therefore, c-OED can reflect the property parameter use in a chemical process simulation directly in the objective, e.g. the impact of NRTL-parameters on the total process energy demand.

Interestingly, c-optimality is mathematically a special case of weighted A-optimality [24]. Thus, c-OED is connected to the modified A-optimal criterion from [21]. In contrast to [21], c-OED weights parameter uncertainties by first-order derivatives instead of scaling the OED problem by second-order derivatives of the Lagrange function of an optimisation problem. Therefore, c-OED is suitable for chemical process simulations, while the method from Houska et al. [21] is tailored to equation-based optimisation problems and requires the Lagrange function of the optimisation problem.

To date, c-optimality has only been applied for the optimal experimental design of clinical trials for dose-finding in the area of toxicology studying [25–27] or the description of viral dynamics and pharmacokinetics [28], but not in chemical engineering for process flowsheet simulation. However, in particular for physical properties for process flowsheet simulations, experiments for parameter estimation serve a purpose beyond the pure parameter knowledge, which needs to be reflected by the OED objective.

In this work, we therefore investigate OED using c-optimality for accurate chemical flowsheet simulations. Preliminary results of this work have been published in a conference paper, in which we discussed heuristically scaled OED for process simulations [20]. Here, we focus on c-OED for chemical engineering problems (Section 2) and demonstrate the benefit of c-OED for extraction and extraction-distillation process models (Section 3). We design experiments for the estimation of parameters for activity coefficient and diffusion models, considering their use in a flowsheet simulation. We compare the c-optimal experimental design with the state-of-the-art OED in chemical engineering for parameter accuracy (D-optimal experimental design) and conventionally used experimental designs without OED. Finally, we validate OED theory by simulation of experiments using Monte-Carlo analysis (Section 4) before concluding this paper for future work.

2. Background and method: optimal experimental design using the c-optimality criterion

In this section, we briefly explain the state-of-the-art theory and fundamentals of OED. We focus on c-OED, which we adapt to the estimation of thermodynamic properties for chemical process simulations. We start with deriving the c-optimal objective function (Section 2.1) before we explain how to solve OED problems (Section 2.2). In Section 2.3, we introduce quality measurement criteria to compare and validate the results in Section 3.

2.1. Derivation of the c-optimal objective function

In general, the goal of statistical OED is to minimize parameter uncertainty. For this purpose, the objective is defined as a measure of the variance-covariance matrix of parameters $\boldsymbol{V}_\theta$. The parameter variance-covariance matrix $\boldsymbol{V}_\theta$ can be approximated by the product of the Fisher-Information-Matrix $\boldsymbol{F}(\hat{\boldsymbol{\theta}}, \boldsymbol{\xi})$ and the number of experiments N_{exp} [29]:

$$\boldsymbol{V}_\theta \approx \left[N_{\text{exp}} \boldsymbol{F}\left(\hat{\boldsymbol{\theta}}, \boldsymbol{\xi}\right) \right]^{-1} \tag{1}$$

As the parameter variance-covariance matrix $\boldsymbol{V}_\theta$ is proportional to the inverse of $\boldsymbol{F}(\hat{\boldsymbol{\theta}}, \boldsymbol{\xi})$, OED usually focuses on optimising the Fisher-Information-Matrix $\boldsymbol{F}(\hat{\boldsymbol{\theta}}, \boldsymbol{\xi})$ by selecting an optimal design $\boldsymbol{\xi}^*$ that contains the distribution of experiments independent from the total number of experiments N_{exp}. The Fisher-Information-Matrix $\boldsymbol{F}(\hat{\boldsymbol{\theta}}, \boldsymbol{\xi})$ depends on the chosen experimental design $\boldsymbol{\xi}$ and an initial parameter guess $\hat{\boldsymbol{\theta}}$ if the model is not linear in the parameters [29]. For example, for OED of phase equilibria measurements to parametrise the NRTL-model [30], an initial set of NRTL-parameters has to be provided.

We represent every experimental design $\boldsymbol{\xi}$ by a design vector of N distinct experimental settings $\boldsymbol{z}_i$, e.g. temperature and pressure of each experiment, and corresponding N normalised weights v_i, which indicate the share of the total experimental effort [24]:

$$\boldsymbol{\xi} = \begin{Bmatrix} \boldsymbol{z}_1 & \boldsymbol{z}_2 & \cdots & \boldsymbol{z}_{\text{N}} \\ v_1 & v_2 & \cdots & v_{\text{N}} \end{Bmatrix} \quad \text{with} \quad \sum_{i=1}^{N} v_i = 1 \tag{2}$$

The number of distinct experimental settings N is usually not known a priori and a result of OED besides the specification of the experimental settings.

The Fisher-Information-Matrix $\boldsymbol{F}(\hat{\boldsymbol{\theta}}, \boldsymbol{\xi})$ is calculated from the underlying model of the experiment $\boldsymbol{g}(\boldsymbol{z}, \boldsymbol{w}, \boldsymbol{\theta})$ [29]. The model $\boldsymbol{g}(\boldsymbol{z}, \boldsymbol{w}, \boldsymbol{\theta})$ describes the experiments by relating the parameters $\boldsymbol{\theta}$ for given experimental settings $\boldsymbol{z}$ to the experimental measurement results $\boldsymbol{w}$. For flowsheet simulation of chemical processes, for example, the model $\boldsymbol{g}(\boldsymbol{z}, \boldsymbol{w}, \boldsymbol{\theta})$ describes the experiments to measure liquid-liquid-equilibria or diffusion experiments. The experiments are characterised by experimental settings $\boldsymbol{z}$ given as input from the experimental design $\boldsymbol{\xi}$, e.g. temperatures and concentrations. The experimental measurements $\boldsymbol{w}$ are, for example, measured phase compositions.

The Fisher-Information-Matrix $\boldsymbol{F}(\hat{\boldsymbol{\theta}}, \boldsymbol{\xi})$ for a given experimental design $\boldsymbol{\xi}$ is calculated by multiplying the variance-covariance matrix of the experimental measurements $\boldsymbol{V}_{\text{w}}$ by the model sensitivity to experimental measurements $\boldsymbol{A}_\mu$ and the model sensitivity to parameters $\boldsymbol{B}_\mu$ for each experiment μ of the experimental design $\boldsymbol{\xi}$ [29]:

$$\boldsymbol{F}\left(\hat{\boldsymbol{\theta}}, \boldsymbol{\xi}\right) = \sum_{\mu=1}^{N} v_\mu \boldsymbol{B}_\mu^T \left(\boldsymbol{A}_\mu \boldsymbol{V}_{\text{w}} \boldsymbol{A}_\mu^T\right)^{-1} \boldsymbol{B}_\mu + \boldsymbol{\Sigma}_0^{-1} \tag{3}$$

with the local model sensitivity to experimental measurements: $\boldsymbol{A}_\mu = \left.\frac{\partial \boldsymbol{g}}{\partial \boldsymbol{w}}\right|_{\boldsymbol{w}_\mu, \hat{\boldsymbol{\theta}}}$ and the local model sensitivity to parameters: $\boldsymbol{B}_\mu = \left.\frac{\partial \boldsymbol{g}}{\partial \boldsymbol{\theta}}\right|_{\boldsymbol{w}_\mu, \hat{\boldsymbol{\theta}}}$

The variance-covariance matrix of the experimental measurements $\boldsymbol{V}_{\text{w}}$ is a key input parameter, which needs to be specified a priori from uncertainty measurements highlighting the need for uncertainty reporting as part of good reporting practice for property measurements [31]. Already available information on the parameter variance-covariance matrix, e.g. from previously performed experiments or the literature, can be included for the design of further experiments in the Fisher-Information-Matrix $\boldsymbol{F}\left(\hat{\boldsymbol{\theta}}, \boldsymbol{\xi}\right)$ through $\boldsymbol{\Sigma}_0$ since $\boldsymbol{F}\left(\hat{\boldsymbol{\theta}}, \boldsymbol{\xi}\right)$ is additive [24]. In this work, no previously performed experiments are assumed; thus, $\boldsymbol{\Sigma}_0^{-1}$ is not further considered.

To account for the parameter use, the c-optimal design objective is to minimise a linear combination of the parameter variances, which is calculated by the product of a vector $\boldsymbol{c}(\hat{\boldsymbol{\theta}})$ and the inverse of the Fisher-Information-Matrix $\left[\boldsymbol{F}(\hat{\boldsymbol{\theta}}, \boldsymbol{\xi})\right]^{-1}$ [4]. The c-optimal experimental design $\boldsymbol{\xi}_{\text{c}}^*$ is the solution to this optimization problem:

$$\boldsymbol{\xi}_{\text{c}}^* = \arg\min_{\boldsymbol{\xi}} \; \boldsymbol{c}(\hat{\boldsymbol{\theta}})^T \left[\boldsymbol{F}(\hat{\boldsymbol{\theta}}, \boldsymbol{\xi})\right]^{-1} \boldsymbol{c}(\hat{\boldsymbol{\theta}}) \tag{4}$$

For considering the property parameter use in a process simulation, $\boldsymbol{c}(\hat{\boldsymbol{\theta}})$ should reflect the linearised variance propagation of the property parameter uncertainties through the process model. Therefore, the first-order sensitivities of a scalar simulation output to property parameters are chosen as weights of the linear combination. Thereby, the property parameters are weighted by their impact on the process model, e.g. the sensitivity of total process energy demand with respect to NRTL-parameters. The variance of a simulation output is thus obtained as c-OED objective. We calculate the vector $\boldsymbol{c}(\hat{\boldsymbol{\theta}})$ from the sensitivities of a scalar result of the process model $h\left(\boldsymbol{\theta}, \boldsymbol{\kappa}\right)$ to property parameters $\boldsymbol{\theta}$:

$$\boldsymbol{c}(\hat{\boldsymbol{\theta}}) = \left.\frac{\partial h\left(\boldsymbol{\theta}, \boldsymbol{\kappa}\right)}{\partial \boldsymbol{\theta}}\right|_{\hat{\boldsymbol{\theta}}, \hat{\boldsymbol{\kappa}}} \tag{5}$$

As both the model sensitivities for the Fisher-Information-Matrix $\boldsymbol{F}(\hat{\boldsymbol{\theta}}, \boldsymbol{\xi})$ and the process model sensitivities for the vector $\boldsymbol{c}(\hat{\boldsymbol{\theta}})$ are calculated for given initial parameters $\hat{\boldsymbol{\theta}}$, the resulting optimal experimental design is locally optimal for the given initial parameters $\hat{\boldsymbol{\theta}}$. The vector $\boldsymbol{c}(\hat{\boldsymbol{\theta}})$ can also depend on further parameters, e.g. specifications of the process model $\boldsymbol{\kappa}$, resulting in an additional dependence of the optimal experimental design on these parameters. These additional specifications, such as operation settings, must be known a priori, e.g. from experience, known operation of similar systems or process design.

In contrast to c-OED, state-of-the-art OED criteria do not consider the process sensitivity to the property parameters expressed by $\boldsymbol{c}(\hat{\boldsymbol{\theta}})$. For example, the commonly used D-optimal experimental design yields the most accurate parameters by using only the Fisher-Information-Matrix. A D-optimal experimental design $\boldsymbol{\xi}_{\mathrm{D}}^{*}$ minimises the uncertainty of all parameters by maximising the determinant of the Fisher-Information-Matrix [29]:

$$\boldsymbol{\xi}_{\mathrm{D}}^{*} = \arg\max_{\boldsymbol{\xi}} \log\left[\det\left(\boldsymbol{F}\left(\hat{\boldsymbol{\theta}}, \boldsymbol{\xi}\right)\right)\right] \tag{6}$$

Generally, statistical OED as presented here requires several assumptions on the model and the errors that have been summarised, e.g. in [29] or [8]: (1) The model parameters $\boldsymbol{\theta}$ need to be identifiable, and the true values for the measurements need to lead to the true parameter values, i.e. no model bias is assumed. (2) No errors are assumed in the independent variables, i.e. the experimental settings $\boldsymbol{z}$, and no systematic errors are assumed in the measured variables $\boldsymbol{w}$. (3) Errors in different experiments are independent of each other and normally distributed with the same covariance matrix $\boldsymbol{V}_{\mathrm{W}}$.

Importantly, the thermodynamic model $\boldsymbol{g}$ and the experimental measurements $\boldsymbol{w}$ need to be carefully selected since multiple options exist for the model and the measured quantities. For example, van Ness and coworkers showed that isobaric vapour-liquid-equilibrium (VLE) measurement usually lead to large uncertainties and model errors in contrast to isotherm VLE experiments [32,33]. Isobaric VLEs rely on vapour pressure equations used as input. If inadequately parametrized, this input can cause a model bias in the temperature dependence of the vapour pressure. The intrinsic model bias then leads to incorrect parameters - independent of the experimental design.

2.2. Solving OED problems

The computation of the OED objectives requires sensitivities. The model sensitivities of the thermodynamic model to experimental measurements and property parameters as well as the sensitivities of the process model to property parameters are calculated by first-order numerical differentiation using central differences. To ensure stable numerical differentiations, we performed a parameter study and chose as the step size of 1×10^{-7} for the calculation of the Fisher-Information-Matrix via imaginary variables [34] and a stepsize of 1×10^{-4} for the sensitivities of the process model.

To solve optimal experimental design problems, several general-purpose algorithms have been proposed in the literature [35]. In this work, we use the general algorithm for computing optimal designs with monotonic convergence by Yu [36].

The algorithm yields optimal experimental designs with a continuous distribution of experimental effort, also called continuous designs [4]. A continuous design quantifies which share of the total experimental effort should be spent on which measurements. Continuous designs suit as targets for experiments in the laboratory, as these designs specify only relative experimental effort for an infinite number of experiments. In practice, only a limited number of experiments can be performed. Therefore, implementable experimental designs for the laboratory, so-called exact designs, can be calculated for a predefined number of experiments, e.g. by rounding the continuous designs [4]. However, as rounding does not guarantee close approximation of continuous designs [4], various algorithms for the calculation of exact designs have been developed, e.g. non-sequential algorithms [37] or exchange methods [38]. In the validation section of this paper, we use a non-sequential algorithm for exact optimal designs as proposed by Wynn [37] (Section 4). Exact designs can also be calculated considering previous experiments or literature data (cf. Eq. (3)), as frequently required in practice. The exact design then yields the optimal subsequent experiments, as demonstrated by [9].

2.3. Comparison of experimental designs

Experimental designs can be compared by OED-efficiencies, which measure the effectiveness of an experimental design $\boldsymbol{\xi}$ compared to an optimal design $\boldsymbol{\xi}^{*}$. In this work, we focus on c-efficiency as a measure of process simulation accuracy and D-efficiency as a measure of parameter accuracy. The efficiencies are defined based on the c-optimal $\boldsymbol{\xi}_{\mathrm{c}}^{*}$ or D-optimal design $\boldsymbol{\xi}_{\mathrm{D}}^{*}$ as [4]:

- c-efficiency: $\zeta_{\mathrm{c}}(\boldsymbol{\xi}) = \dfrac{\boldsymbol{c}(\hat{\boldsymbol{\theta}})^{T}\boldsymbol{F}(\hat{\boldsymbol{\theta}}, \boldsymbol{\xi}_{\mathrm{c}}^{*})^{-1}\boldsymbol{c}(\hat{\boldsymbol{\theta}})}{\boldsymbol{c}(\hat{\boldsymbol{\theta}})^{T}\boldsymbol{F}(\hat{\boldsymbol{\theta}}, \boldsymbol{\xi})^{-1}\boldsymbol{c}(\hat{\boldsymbol{\theta}})}$
- D-efficiency: $\zeta_{\mathrm{D}}(\boldsymbol{\xi}) = \left[\dfrac{\det\left(\boldsymbol{F}\left(\hat{\boldsymbol{\theta}}, \boldsymbol{\xi}\right)\right)}{\det\left(\boldsymbol{F}\left(\hat{\boldsymbol{\theta}}, \boldsymbol{\xi}_{\mathrm{D}}^{*}\right)\right)}\right]^{\frac{1}{n_{\mathrm{parameter}}}}$

with $n_{\mathrm{parameter}}$ for the number of estimated model parameters. The efficiencies are valuable metrics since they allow to determine the number of experiments to achieve a particular accuracy. The inverse of the c- or D-efficiency describe how many experiments are additionally required for the same accuracy compared to an optimal design of the respective criterion. For example, a design with a c-efficiency $\zeta_{\mathrm{c}} = 0.25$ needs 4 times as many experiments for the same process simulation accuracy than a c-optimal design.

3. Case studies

The c-OED is applied by computing continuous c-optimal experimental designs for liquid-liquid-equilibrium and diffusion experiments for two process models of solvent-based processes as an example:

1. Pinch-based process models for extraction and distillation [39,40]

2. Countercurrent rate-based extraction model with the HTU-NTU model for sizing [41,42]

In both case studies, the thermodynamic model for liquid-liquid-equilibrium measurements is taken from [8] and uses the NRTL activity coefficient model [30]. For the HTU-NTU sizing of the extraction column, diffusion coefficients are additionally required and assumed to be measured using a closed cell with fixed geometries as the experimental setup [10].

We exemplify c-OED in this paper for the ternary system water-acetone-toluene in both case studies. We limit the study to ternary systems for ease of interpretation and visualisation. However, the method of c-OED is not limited to ternary systems but is applicable for multi-component systems with more than three components.

The chemical system water-acetone-toluene is a model system of great interest in research and industry since it is applicable for studying various processes such as extraction and distillation [43]. The components represent a variety of chemical interactions: Water and toluene are almost completely immisci-ble since water is a highly polar molecule, whereas toluene is highly unpolar. Acetone is mildly polar and, thus, soluble in both water and toluene. Toluene is consequently a suitable solvent for the extraction of acetone from water since only acetone is attracted to the extract toluene phase leading to a selective separation. Therefore, the system is well suited to study the estimation of binary interaction parameters for extraction and extraction-distillation processes.

We compare the continuous c-optimal experimental designs as targets for maximum experimental efficiency with state-of-the-art OED for maximum parameter precision (D-optimal experimental design) and a conventional experimental design without OED, which equally distributes the experimental effort over the design space. Numerical details on the experimental designs and the initial property parameters for each design can be found in the Supporting Information.

3.1. Pinch-based process models for extraction and distillation

For the pinch-based process models, we investigate two process flowsheets: (1) An isothermal extraction modelled by one extraction column and (2) a hybrid extraction-distillation modelled by an extraction column followed by a distillation column. The goal for OED is to provide optimal liquid-liquid equilibrium measurements to estimate isothermal NRTL-parameters for the extraction process and temperature-dependent NRTL-parameters for the extraction-distillation process.

3.1.1. OED for estimation of isothermal NRTL-τ-parameters for an extraction column

As the first case study, we investigate the extraction of acetone from aqueous solution at 25 °C using toluene as a solvent. The extraction column is modelled using a pinch-based process model, taking NRTL-parameters as input [40]. Pinch-based process models assume infinite columns operating at vanishing thermodynamic driving force but consider the full non-ideal thermodynamics. Therefore, the model yields the minimum solvent demand $S_{\min}$ required for this separation. In particular, for the selection of an extraction solvent, the minimum solvent demand characterises the extraction process as the performance metric h.

We aim to determine the minimum solvent demand $S_{\min}$ for extraction as accurately as possible. For this purpose, we use OED to decide which LLE experiments should be performed to estimate the six NRTL-τ-parameters for the binary interactions. LLE experiments are typically performed by equilibrating a liquid mixture with known overall composition and miscibility gap in an equilibrium cell. After equilibration, samples are drawn from each liquid phase and the molar composition of each phase is measured. Today, mixing, equilibration, sample drawing and measuring is preferably integrated in an automated set-up [44–46].

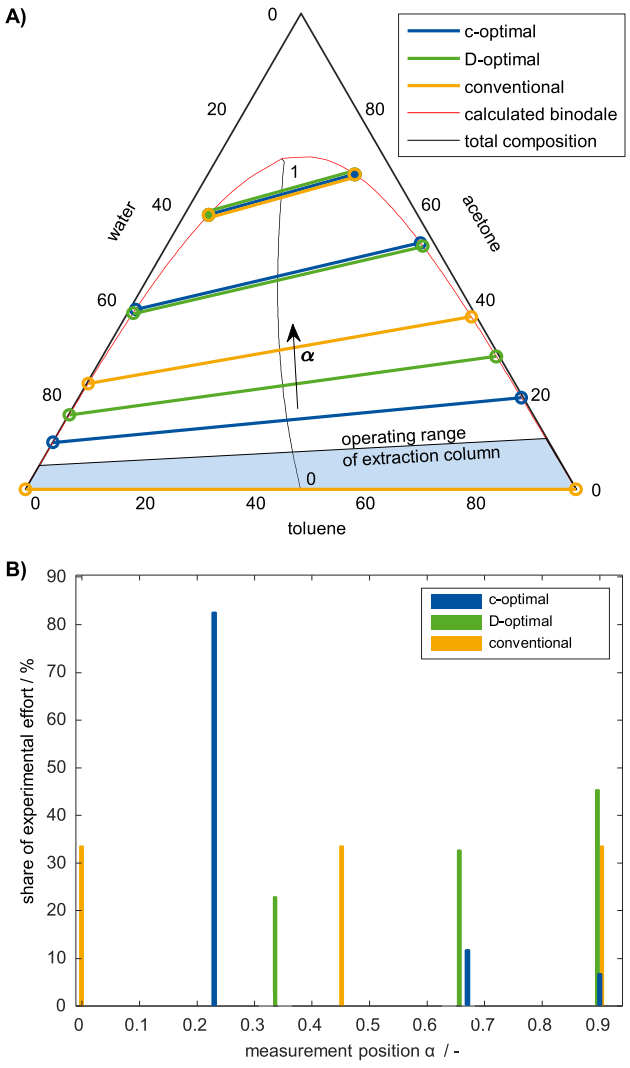

Fig. 1. Experimental designs for LLE experiments for the extraction process: (A) Location of LLE experiments. (B) Share of experimental effort. Part A of the figure also shows the scalar quantity α, which characterises the centre of the tie lines and the total composition of an experiment.

For simplicity, we assume that LLE experiments are performed with the overall composition of the components that corresponds to the centre of the tie lines. The overall compositions of all experiments lie on a line running from the center of the miscibility gap of the binary subsystem to the critical point (cf. Fig. 1A). Each position on this line is labeled by the scalar quantity α defined linearly from the beginning in the binary subsystem ($\alpha = 0$) to the end at the critical point ($\alpha = 1$), which thus defines each experiment exactly [8]. As a result, the three-dimensional representation of the overall composition of the experiment is precisely described by the parameter α, without simplifying the problem. Measurements are challenging close to the critical point. In addition, the NRTL model is known to describe the phase equilibrium poorly close to the critical point, leading to model bias. To ensure experimental feasibility and applicability of the NRTL-model, we limit α to a maximum of 0.9. Since we investigate ternary mixtures in this work, two molar fractions are measured for each experiment and each liquid phase (cf. thermodynamic model of LLE experiments by Dechambre et al. [8]). For each measurement, we assume the same constant measurement uncertainty $\sigma_w = 0.005$ (cf. Section 4).

Table 1
c- and D-efficiencies ζ_c and ζ_D of the c-optimal $\boldsymbol{\xi}_c^*$, D-optimal $\boldsymbol{\xi}_D^*$ and equidistantly distributed conventional $\boldsymbol{\xi}_{con}$ experimental designs for the estimation of isothermal NRTL-τ-parameters and use in the pinch-based extraction process model.

Design $\boldsymbol{\xi}$	c-efficiency ζ_c	D-efficiency ζ_D
c-optimal $\boldsymbol{\xi}_c^*$	1	0.44
D-optimal $\boldsymbol{\xi}_D^*$	0.36	1
conventional $\boldsymbol{\xi}_{con}$	0.10	0.56

The c-optimal experimental design selects three distinct locations for measurements (Fig. 1B). About 80 % of the experimental effort is placed near the operating range of the extraction column at $\alpha = 0.22$. However, no experiments are performed in the actual operating range of the extraction column. Instead, 20 % of the experimental effort is placed in the high-curvature region of the binodal curve at $\alpha > 0.65$, in particular, 6 % at the design space boundary at $\alpha = 0.9$. Thus, the c-optimal experimental design provides another argument to support the previous conclusions that the process operation settings should not be mimicked or copied for for physical property experiments [32].

The D-optimal experimental design similarly focuses on three distinct locations for measurements. However, in contrast to the c-optimal design, 65 % of the experiments are placed in the high-curvature region of the binodal curve, as already discovered by Dechambre et al. [8]. In the high-curvature region of the binodal curve, the phase equilibrium model is highly sensitive to the property parameters. Thus, placing experiments in the high-curvature region leads to low uncertainty in the parameter estimation. However, the c-efficiency of the D-optimal design is only $\zeta_c^D = 0.36$ (Table 1). Consequently, about three times more D-optimal than c-optimal experiments are required to achieve the same accuracy in the process simulation.

For an equidistantly distributed conventional experimental design, we specify three experimental settings since the c- and D-optimal designs yielded three distinct settings. The experimental effort is equally distributed across all experiments. The conventional design yields a low c-efficiency of only $\zeta_c^{con} = 0.10$ despite placing experimental effort within the operating range of the extraction column in the solvent-carrier binary subsystem. As a result, the conventional design requires about ten times more experiments for the same process simulation accuracy as the c-optimal design. Thus, the c-optimal experimental design promises to achieve a significant reduction in experimental effort.

In terms of parameter precision, the c-optimal design scores a D-efficiency of $\zeta_D^c = 0.44$. In contrast, the conventional design yields a D-efficiency of $\zeta_D^{con} = 0.56$ and, thus, returns more accurate parameter values than the c-optimal design. The low D-efficiency of the c-optimal design illustrates the varying influence of each property parameter on simulation accuracy. For the extraction process, not all parameters of the thermodynamic model are equally important. For example, the binary interactions between solvent and solute as well as carrier and solute are of major importance. However, the simulation results are much less sensitive to the solvent-carrier interaction parameters, although low miscibility between solvent and carrier resulting from the solvent-carrier interactions is key for the extraction process. Nevertheless, highly accurate estimation of the solvent-carrier interaction is not required for accurate process simulations since small inaccuracies in the solvent-carrier interaction parameters still lead to low miscibility between solvent and carrier. Therefore, spending additional experimental effort on increasing the parameter precision of these less important parameters for the simulation reduces c-efficiency. Instead, the experimental effort is more efficiently spent on experiments targeting the more influential property parameters of the simulation. For example, near the operating range of the extraction column, the thermodynamic model of the LLE experiments is most sensitive to solvent-solute interaction, while the sensitivity to solvent-carrier interactions is low. Therefore, the c-optimal design places the majority of the experimental effort on the experimental settings near the operating range. However, exclusive focus on the property parameters most important for the chemical process simulation neglects the accuracy increase resulting from experiments for overall high parameter precision. Therefore, the c-optimal design also includes experiments for overall parameter accuracy such as experiments in the high-curvature region of the binodal curve at $\alpha = 0.9$.

3.1.2. OED for estimation of temperature-dependent NRTL-τ-parameter from LLE experiments for a hybrid extraction-distillation process

As the second case study, we extend the extraction process from Section 3.1.1 by a distillation column. First, acetone is extracted from the aqueous solution using toluene before acetone is separated from the extract using distillation. Both the extraction and distillation columns are modelled using a pinch-based process model [39,40]. For this case study, the key performance metric h is the minimum reboiler energy demand of the distillation column Q_{min} that we want to estimate as accurately as possible. We estimate two isothermal and two temperature-dependent NRTL-τ-parameters for each binary interaction pair because of the temperature gradient in the distillation column. Therefore, in this case study, c-OED is used to determine at which temperatures and concentrations LLE experiments should be performed to calculate the minimum reboiler energy demand Q_{min} as accurately as possible. For the demonstration of the c-OED, we limit the designed experiments to LLE-experiments. In practice, however, the NRTL parameters should be estimated through liquid-liquid -and vapour-liquid-equilibrium experiments for higher accuracy [47]. As in Section 3.1.1, we limit the design space to concentrations corresponding to $\alpha < 0.9$ to ensure experimental feasibility and applicability of the NRTL-model, and now also consider a temperature range of 10–80°C.

The experimental designs consist of a non-trivial combination of nine experimental settings for the c-optimal and eight for the D-optimal design across the whole design space (Fig. 2). Both the c- and D-optimal experimental designs mainly focus on the boundaries of the design space but avoid experiments at and near the binary subsystem of solvent and carrier with $\alpha < 0.2$ (Fig. 2). At the boundaries, where temperature is high or near the critical point at high α, the thermodynamic model is particularly sensitive to the property parameters reducing parameter uncertainty more than in the centre of the design space. The binary subsystem is avoided for all temperatures since both isothermal and temperature-dependent parameters are more accurately estimated in the high-curvature region of the binodal curve (cf. Section 3.1.1).

The c-optimal design favours experiments at lower α than the D-optimal design as already discovered in the isothermal case study (Section 3.1.1), e.g. the total experimental effort spent in the c-optimal design for $\alpha < 0.6$ equals 56 %. At low α, the binary interactions between solvent and solute as well as carrier and solute can be more accurately determined, which is crucial for a high process simulation accuracy. In contrast, the D-optimal design places only 27 % of the total experimental effort on measurements with $\alpha < 0.6$. Similarly to the estimation of isothermal NRTL-parameters, experiments at higher α are important for higher parameter precision.

To capture the temperature dependency accurately, the c-optimal design places a large share of the experimental effort at experiments with higher temperatures: 78 % of the total experimental effort is spent for temperatures higher than 60 °C. The fo-

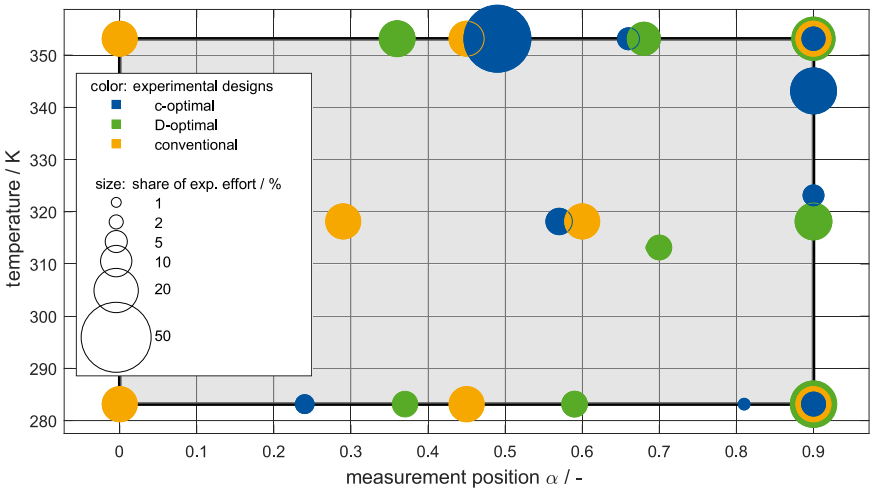

Fig. 2. Experimental designs for LLE experiments for the extraction-distillation process. The size of the circles corresponds to the share of the experimental effort. The grey box indicates the design space.

Table 2
c- and D-efficiencies ζ_c and ζ_D of the c-optimal $\boldsymbol{\xi}_c^*$, D-optimal $\boldsymbol{\xi}_D^*$ and equidistantly distributed conventional $\boldsymbol{\xi}_{con}$ experimental designs for the estimation of temperature-dependent NRTL-τ-parameters and use in the pinch-based extraction-distillation process model.

Design $\boldsymbol{\xi}$	c-efficiency ζ_c	D-efficiency ζ_D
c-optimal $\boldsymbol{\xi}_c^*$	1	0.62
D-optimal $\boldsymbol{\xi}_D^*$	0.61	1
conventional $\boldsymbol{\xi}_{con}$	0.24	0.55

cus on higher temperatures in the c-optimal design can be explained by the temperature glide from the condenser ($T_{cond} = 74\,^\circ$C) to the reboiler ($T_{reb} = 110\,^\circ$C) in the distillation column. For an accurate description of distillation, capturing the temperature dependence of the NRTL parameters is important, and at higher temperatures, the temperature-dependent parameters are more sensitive to the measurements.

The D-optimal design only allocates 43 % of the experimental effort for temperatures higher than 60 °C to balance the estimation of isothermal and temperature-dependent NRTL-parameters resulting in a c-efficiency of $\zeta_c^D = 0.61$ (Table 2). Compared to the D-optimal design for isothermal NRTL-parameters in Section 3.1.1, the c-efficiency of the D-optimal design increases by 69 %. Therefore, for the extraction-distillation process, parameter precision is generally more important for accurate process simulation than for the extraction only. As a result, parameter precision as measured by the D-efficiency also increases to $\zeta_D^c = 0.62$ for the c-optimal design by about 40 % compared to the c-optimal design for isothermal NRTL-parameters.

For the conventional design, we assume equally distributed experimental effort on eight experimental settings across the design space (Fig. 2). As in the first case study (Section 3.1.1), the optimal experimental designs significantly outperform the conventional design in both process simulation and parameter accuracy ($\zeta_c^{con} = 0.24$ and $\zeta_D^{con} = 0.55$, Table 2) emphasising the benefits of OED. In particular, the c-optimal experimental design is predicted to reduce experimental effort by 75 % compared to the conventional design for the same process simulation accuracy. Therefore, manually distributing the experimental effort across a large design space is particularly inefficient for subsequent use of the property parameters in a process simulation.

3.2. Countercurrent rate-based extraction column with HTU-NTU sizing

As the third case study, we again consider the extraction of acetone from aqueous solution at 25 °C using toluene as a solvent based on the Ph.D. thesis by Wolff [48]. However, in contrast to Case Study 1 (Section 3.1.1), we use a countercurrent rate-based extraction model with HTU-NTU sizing instead of a pinch-based process model. The countercurrent extraction column assumes mass transfer of the solute only, following two-film theory with a constant mass transfer coefficient and thermodynamic equilibrium at the interface. In contrast to the pinch-based process models, we include sizing using the HTU-NTU method [41,42] and costing [49] (see SI for detailed equations). Therefore, the final model result is the total annualised cost (TAC), which should be determined as accurately as possible using c-OED.

As a consequence, the model needs both isothermal NRTL-τ- and diffusion parameters as property data. Therefore, we extend the OED to the selection of experiments for several thermodynamic properties. The optimal experimental design not only yields which LLE and diffusion experiments to perform but also balances the experimental effort between LLE and diffusion experiments. Thus, the design vector of experiments $\boldsymbol{\xi}$ includes the scalar measure α of LLE-experiments and additionally the effort on experiments for the diffusion coefficients of acetone in water D_W and acetone in toluene D_T.

The diffusion experiments are assumed to be performed in a closed diffusion cell filled with equal volumes of two substances. The diffusion coefficients are derived from concentration measurements using Fick's second law. Here, we assume measurements at one position δ in the closed cell and at one dimensionless measurement time given by the Fourier number Fo [10]. Therefore, the OED methodology determines the optimal Fourier number Fo^* and the optimal measurement position δ^*. For the calculations, a standard deviation of $\sigma_w = 0.5\%$ is assumed in measuring the phase compositions in the LLE experiments and the concentrations in the diffusion experiments.

For the LLE experiments, c-optimal design selects the same three measurements with the same relative distribution of experimental effort among the LLE experiments as the OED for the pinch-based process model for extraction in Section 3.1.1 (cf. Fig. 1). Therefore, the dominating interactions for describing the

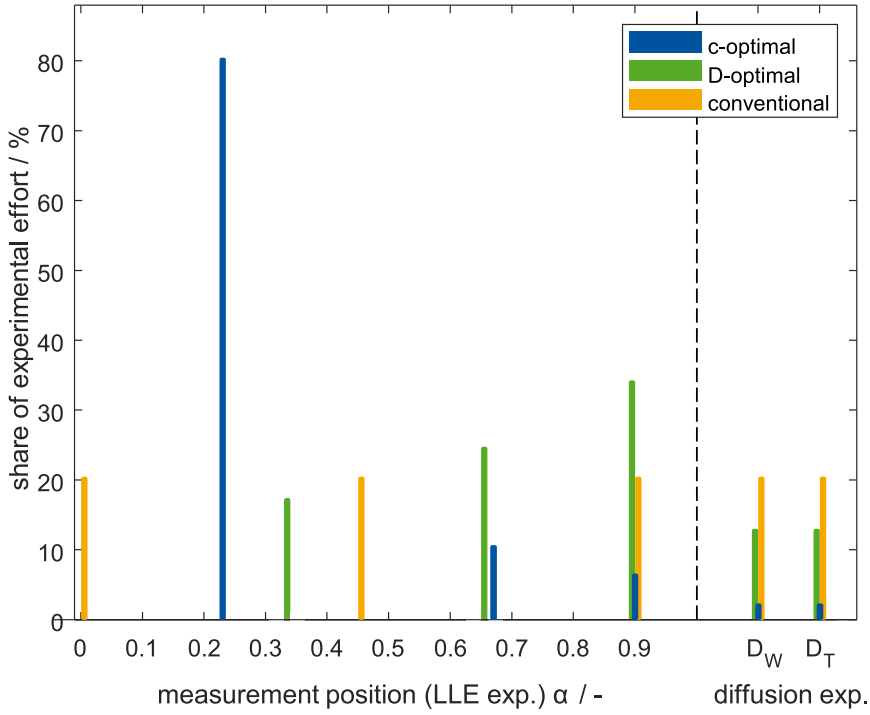

Fig. 3. Experimental designs for LLE and diffusion experiments for the extraction model using the HTU-NTU approach.

minimum solvent demand using the pinch-based process model are also most important for the countercurrent rate-based extraction model. The selection of the same experimental settings is reasonable since both process models use the same thermodynamic model describing the liquid-liquid equilibrium as a basis for the solvent demand and cost calculations. Therefore, a precise description of the extraction process is a prerequisite for accurate cost calculation. Naturally, the D-optimal design equals the D-optimal design in Section 3.1.1 if focusing only on the LLE experiments since the same thermodynamic model describing the experiments is considered.

The diffusion experiments have the same optimal design using either c- or D-OED: The most accurate estimation of diffusion coefficients is achieved at a Fourier number $Fo^* = 0.1$ and the measurement position $\delta^* = 0$, i.e. at the wall of the closed diffusion cell. Moreover, the experimental effort is equally distributed between the diffusion coefficients of acetone in water D_W and acetone in toluene D_T for both designs (cf. Fig. 3).

However, the designs differ strongly in the distribution of experimental effort between LLE and diffusion experiments: The c-optimal design focuses 96 % of the total experimental effort on LLE experiments and only 4 % on the diffusion experiments. Therefore, the property parameters describing the phase behaviour are more important for accurate process simulation and costing than the parameters describing the diffusion. In contrast, the D-optimal design places 25 % of the experimental effort on diffusion experiments and yields a c-efficiency $\zeta_c^D = 0.46$ (Table 3). Compared to D-optimal design in Case Study 1, the c-efficiency of the D-optimal design improves since the D-optimal design selects the same optimal diffusion experiments as the c-optimal design. The process simulation accuracy benefits more from performing the optimal diffusion experiments than from LLE experiments that are suboptimal for the process model accuracy. Still, the D-optimal design doubles the experimental effort compared to the c-optimal design.

In terms of parameter accuracy, the limited experimental effort on diffusion experiments in the c-optimal design results in low expected accuracy of the diffusion coefficient estimation. As a result, the D-efficiency of the c-optimal design is only $\zeta_D^c = 0.39$.

Table 3
c- and D-efficiencies ζ_c and ζ_D of the c-optimal $\boldsymbol{\xi}_c^*$, D-optimal $\boldsymbol{\xi}_D^*$ and equidistantly distributed conventional $\boldsymbol{\xi}_{con}$ experimental designs estimation of isothermal NRTL-τ-and diffusion parameters and use in the countercurrent rate-based extraction process model.

Design $\boldsymbol{\xi}$	c-efficiency ζ_c	D-efficiency ζ_D
c-optimal $\boldsymbol{\xi}_c^*$	1	0.39
D-optimal $\boldsymbol{\xi}_D^*$	0.46	1
conventional $\boldsymbol{\xi}_{con}$	0.11	0.62

For the conventional experimental design, we manually allocate 60 % of the experimental effort on three equally weighted and distributed LLE experiments as in Section 3.1.1. The remaining 40 % of the experimental effort is equally distributed between the two diffusion experiments. We assume that the optimal settings with $Fo^* = 0.1$ and $\delta^* = 0$ are also selected for each diffusion experiment in the conventional design as these settings have been disclosed in our previous work [10]. As a result, the conventional design yields c- and D-efficiencies of $\zeta_c^{con} = 0.11$ and $\zeta_D^{con} = 0.62$. Similarly to Case Study 1, the conventional design has a substantially lower c-efficiency than the D-optimal design but a comparable D-efficiency to the c-optimal design. Both the c- and D-efficiencies of the conventional design increase by 10 % compared to Case Study 1. Similar to the D-optimal design, the conventional design benefits from the optimal diffusion experiments, which increases both the overall accuracy of parameter estimation and process simulation results.

4. Discussion: uncertainties resulting from the experimental designs

In this section, we challenge the predictions from OED theory by Monte-Carlo analysis for the pinch-based process models of extraction and extraction-distillation since these two case studies ex-

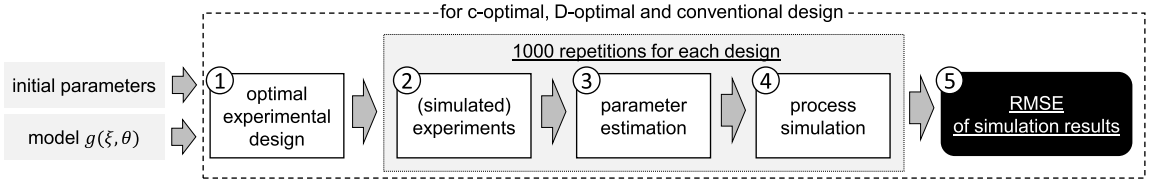

Fig. 4. Procedure for determining the uncertainties of the process simulation results for each experimental design.

hibit the minimum and maximum difference in c-efficiencies reported in this paper. In c-OED theory, the standard deviation of the process simulation result is predicted assuming linear variance propagation. However, process models are usually highly nonlinear. Therefore, assuming linear variance propagation from experiments through parameter estimation and process model only approximates the actual variance propagation. Here, we compare the uncertainty from linear variance propagation in c-OED with propagation from uncertain experimental measurements using a Monte-Carlo approach. For this purpose, we simulate LLE experiments by calculating phase compositions using the initial property parameters (see SI) and adding normally distributed noise to account for measurement errors. Afterwards, we estimate property parameters from the simulated experiments and run the process simulation using the estimated parameters to obtain the actual process model uncertainty. In detail, we apply the following five-step procedure (Fig. 4):

1. *Design optimal experiments*: First, we calculate exact c- and D-optimal designs for a predefined number of experiments using a non-sequential algorithm [37]. Since the resulting exact designs depend on the initialisation of the algorithm, we run the algorithm repeatedly from random starting points to aim for a globally optimal solution. We also create a conventional design, which equidistantly distributes the same number of experiments across the design space.
2. *Simulate experiments*: From the initial property parameters and the thermodynamic model of the LLE experiments, we calculate the phase compositions that result from the experimental designs of Step 1. For this purpose, we assume that the initial property parameters lead to the true phase compositions. Subsequently, we add measurement errors to the true phase compositions by sampling from a Gauss distribution with mean zero and a standard deviation corresponding to typical uncertainty for phase compositions in LLE measurements published in the literature. The typical standard deviation for measuring molar fractions σ_w ranges between 0.001 [50,51] and 0.005 [45,46,52], depending on the measurement method. In this work, we choose a standard deviation $\sigma_w = 0.005$, as higher uncertainties are more challenging for the experimental design methodology because of the assumption of locally optimal designs. For comparison, we also performed Monte Carlo analyses for $\sigma_w = 0.001$ and $\sigma_w = 0.01$, which can be found in the Supporting Information.
3. *Estimate property parameters*: From the simulated experiments, we estimate the property parameters by fitting the thermodynamic model of the LLE experiments. For this purpose, we use the MATLAB solver lsqcurvefit [53] considering 10 starting points for each fit to aim for a globally optimal solution. The direct use of global optimization methods as proposed by Mitsos et al. [54] would be a promising extension for future work.
4. *Calculate process simulation*: We use the estimated property parameters as input for the process simulation to obtain the actual propagation of the estimated property parameters on the process simulation result.
5. *Calculate uncertainty of process simulation*: We repeat steps 2-4 until 1000 process simulation results are obtained for each experimental design. From the 1000 simulation results, we calculate the root mean square error (RMSE) between the simulation results of the estimated parameters from Monte Carlo analysis and the simulation result of initial parameters for each design. The RMSE of the Monte Carlo samples is compared to the expected uncertainty from linear error propagation given by the standard deviation of OED theory. Both the RMSE and the standard deviation are normalized by the actual value of the process simulation result to allow for relative comparisons.

4.1. Accuracy of the extraction process simulation

We investigate the accuracy of the extraction process simulation depending on the experimental design by estimating the six isothermal NRTL-τ-Parameters of the ternary system for 5, 7, 10, 15 and 20 LLE experiments as an example. We measure the uncertainty of the process simulation by computing the relative RMSE of the minimum solvent demand resulting from the pinch-based process model. Generally, the uncertainty of the process simulation results is low, with a relative RMSE of 2–6 % (Fig. 5). Therefore, a small number of experiments, e.g. 5 to 10, is already sufficient for an accurate description of the extraction process.

The predictions from linear variance propagation using the c-optimal objective function (hatched bars) and Monte Carlo analysis (full bars) agree well for each design. The c-optimal objective function successfully predicts qualitatively and quantitatively the uncertainties of the simulation results: For the investigated numbers of experiments, the c-optimal design yields the lowest uncertainty in the Monte Carlo analysis as predicted, followed by the conventional and the D-optimal design. For each experimental design, the relative RMSE decreases monotonically with an increasing number of experiments, as expected from OED theory (cf. Eq. (1)). Thus, for the simulation of the extraction process, Monte Carlo analysis confirms the benefits promised by c-OED theory on simulation accuracy.

Notably, the exact conventional designs with 5–20 experiments yield c-efficiencies between 0.43 and 0.46 and thus, exceed the c-efficiencies of the continuous conventional designs with only three distinct experimental settings (cf. Section 3.1.1). Therefore, the exact conventional designs outperform the exact D-optimal designs in simulation accuracy for this example. The differences in c-efficiency compared to Section 3.1.1 result from the differences between continuous and exact conventional designs and are correctly reflected by the c-optimal objective function.

4.2. Accuracy of the extraction-distillation process simulation

For the hybrid extraction-distillation process, we estimate the six isothermal and six temperature-dependent NRTL-τ-parameters of the ternary system by performing 20, 25, 30, 40 or 50 experiments. We choose more experiments than for the extraction process to capture the temperature dependence with additional parameters. The uncertainty of the process model is measured by the

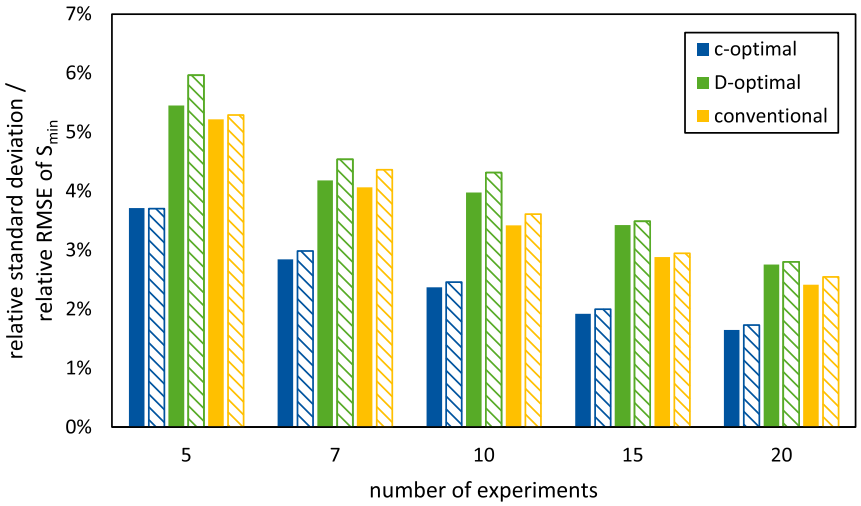

Fig. 5. Uncertainties of the solvent demand of the extraction process for c- and D-optimal and conventional experimental designs. The full bars are the relative RMSE from the Monte Carlo sampling; the hatched bars are the expected relative standard deviation from OED theory.

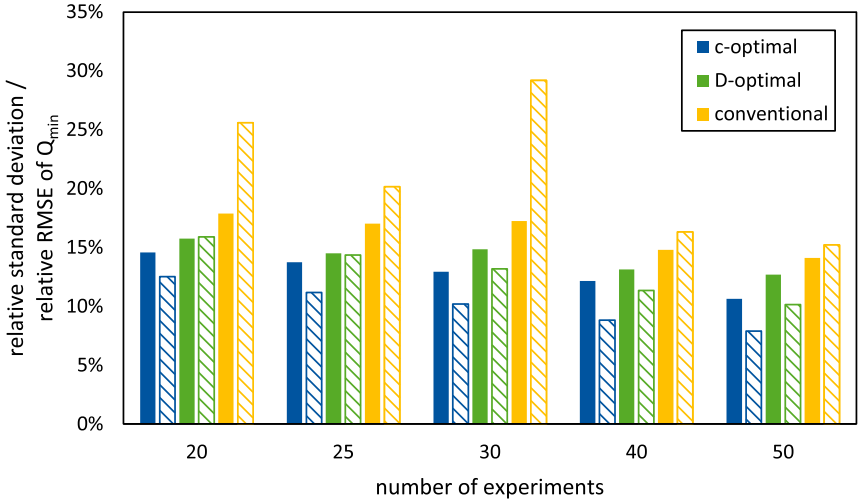

Fig. 6. Uncertainties of the energy demand of the extraction-distillation process for c- and D-optimal and conventional experimental designs. The full bars are the relative RMSE from the Monte Carlo sampling; the hatched bars are the expected relative standard deviation from OED theory.

relative RMSE of the minimum reboiler energy demand resulting from the pinch-based process models.

The relative RMSE of the simulation result range between 10–17 % for the Monte Carlo analysis (full bars, Fig. 6) and are thus about one order of magnitude higher for the extraction-distillation with temperature-dependent NRTL-parameters compared to the extraction with isothermal NRTL-parameter. Qualitatively, the results from the Monte Carlo analysis agree with the ranking obtained from OED theory: The c-optimal design provides the lowest uncertainty in process simulation results, followed by the D-optimal and the conventional design. However, the results from the Monte Carlo analysis deviate quantitatively from OED theory: For the investigated c-optimal designs, the OED theory underestimates the actual uncertainty of process simulation results by up to 38 % of the predicted uncertainty. In contrast, for the investigated conventional designs, the OED theory overestimates the actual uncertainty of the process simulation results by up to 69 % of the actual uncertainty. The predictions for the D-optimal designs match well with the Monte Carlo analysis for 20 and 25 experiments. For 30, 40 and 50 experiments, however, the predictions for the D-optimal designs are increasingly overestimated by up to 25 % of the predicted uncertainty. The results indicate that the assumption of linear error propagation is limited. The improvements predicted by linear variance propagation for c-OED cannot always be achieved. However, c-OED still proves to provide the most accurate simulation results.

In contrast to the c-optimal design, the relative RMSE of the D-optimal design from the Monte Carlo sampling is not always underestimated by OED theory. For fewer experiments, i.e. 20 experiments, the D-optimal design yields a lower uncertainty in the Monte Carlo analysis than predicted by OED theory. Therefore, the accuracy improvement of the c-optimal design decreases compared to the D-optimal design and eventually disappears for the extraction-distillation process if only a minimum number of experiments is performed (cf. analysis in the SI). Thus, for a small number of experiments, an improvement in simulation accuracy cannot be guaranteed by c-OED.

For these experiments, the accuracy increase in the process simulation through c-OED is counterbalanced by the impact of inaccurate property parameters. The property parameter accuracy of

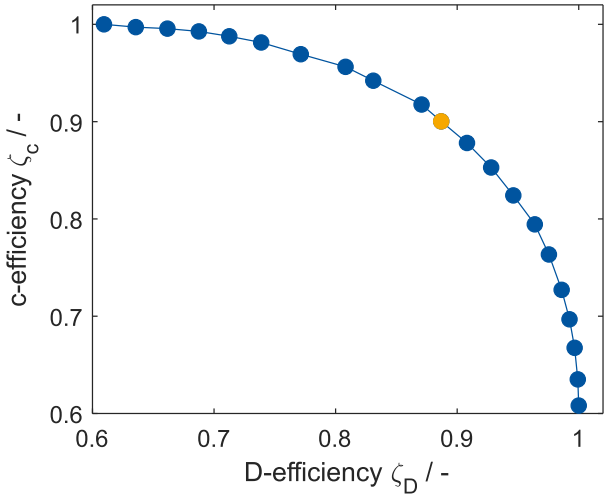

Fig. 7. Pareto frontier between c- and D-efficiency for parameter estimation of the extraction-distillation process. The orange circle marks the trade-off solution with minimum distance from the utopia point ($\zeta_D^{uto} = \zeta_c^{uto} = 1$).

c-OED is lower since overall parameter precision is not the goal of c-OED. Thus, the parameters from c-optimal experiments are more prone to measurement uncertainties and more strongly affected by inaccurate measurements for a small number of experiments.

However, if the number of experiments is increased beyond the minimal number, c-optimal design outperforms the D-optimal and conventional designs. The c-optimal design monotonically decreases in simulation uncertainty, which is not guaranteed for the D-optimal and conventional design. For higher uncertainties in mole fraction measurements, e.g. $\sigma_w = 0.01$, the same qualitative trend can be observed (see analysis in the SI).

In conclusion, the property parameters should be tailored for use in a process simulation but the overall parameter accuracy cannot always be ignored to obtain accurate and robust simulation results. Since the parameters estimated from c-OED are tailored to a specific process, these parameters are not optimal for every purpose. If the parameters are not only used for process simulation but also for, e.g. gaining thermodynamic insights, the OED objective needs to be adapted.

A single OED optimality criterion rarely leads to optimal parameters for all purposes since the individual OED objectives conflict with each other. For the extraction-distillation process, e.g. c- and D-efficiency form a well-defined Pareto frontier (Fig. 7). Neither c-efficiency nor D-efficiency of an optimal multi-objective design can be improved without deteriorating the efficiency of the other objective. Therefore, a multi-objective design needs a carefully balanced optimality criterion. However, the Pareto frontier shows good trade-off solutions: c-efficiency for accurate process simulations can be substantially increased with small losses to the D-efficiency representing parameter accuracy. E.g. a trade-off point minimizing the distance to the utopia point ($\zeta_D^{uto} = \zeta_c^{uto} = 1$) retains a D-efficiency of $\zeta_D^{to} = 0.89$ while increasing c-efficiency from $\zeta_c^D = 0.6$ to $\zeta_c^{to} = 0.9$. The study of such trade-offs could be a valuable use of the introduced c-efficiency concept.

In future work, the parameter precision of the c-optimal design can further be considered towards more robust designs for parameter estimation, e.g. by compound design [24] such as combined c- and D-optimal design [55], or by introducing a minimum D-efficiency as a constraint within the optimisation [26,27]. Methods from the area of robust experimental design can also be explored to strengthen the c-optimal design for reliable improvement of simulation accuracy, e.g. by considering the most inaccurate process simulation as objective for OED [56].

5. Conclusion

In this paper, we introduced c-optimal experimental design (c-OED) as a method of optimal experimental design for chemical engineering problems. c-OED minimises the uncertainty of the process simulation result instead of parameter precision as the design objective. Thus, c-OED considers the application of estimated property parameters in a process simulation already during the design of experiments. To estimate the uncertainty of the process simulation results, c-OED uses linear variance propagation from uncertain property parameters through the process model.

We demonstrate c-OED for estimating isothermal and temperature-dependent NRTL-parameters from liquid-liquid equilibrium experiments for an extraction column and an extraction-distillation process modelled by pinch-based process models. The LLE experiments are designed to minimise the uncertainty of the main thermodynamic performance measures: the minimum solvent demand of the extraction and the minimum energy demand of the extraction-distillation process. Moreover, for a rate-based extraction column sized by the HTU-NTU model, we simultaneously design liquid-liquid equilibrium and closed-cell diffusion experiments that minimise the uncertainty of the total annualised cost of the extraction column.

The application of c-OED for chemical processes shows that considering the sensitivity of the process within OED highly impacts the selection of experiments for property parameter estimation. c-OED yields non-trivial experimental designs that outperform state-of-the-art OED in accuracy of process simulation results. The c-optimal experiments focus on the accurate estimation of parameters most relevant for accurate process simulations. The prioritisation of experiments for specific parameters is particularly evident in the simultaneous design of LLE and diffusion experiments: The major experimental effort of the c-optimal design for the rate-based extraction column is spent on LLE instead of diffusion experiments.

Compared to state-of-the-art OED, c-OED reduces the experimental effort by up to 64 % for the same accuracy in our case studies. Conventionally designed experiments without using OED would increase the experimental effort compared to c-OED by up to a factor of 10, highlighting the need for (c)-OED.

The predictions on accuracy from c-OED theory are examined by Monte Carlo Analysis to challenge the linear approximation of variance propagation. Generally, the OED predictions agree well with the results from Monte Carlo Analysis, and thus, the assumption of linear variance propagation is a good approximation of the actual variance propagation. In our case studies, process simulation accuracy significantly increases through c-OED. The uncertainty of process model results decreases by 30–40 % for an extraction process and by 5–25 % for an extraction-distillation process compared to conventional experimental designs and state-of-the-art OED that does not consider the process. Therefore, c-OED increases accuracy even for highly nonlinear process models and is thus successfully shown to tailor experiments for thermodynamic properties to process simulations.

For future work, the focus should be directed to strengthening the robustness of the c-optimal design, e.g. by compound design [24]. The predictions from c-OED theory can fail due to overall inaccurate property parameters if too few experiments are considered. The c-optimal experimental designs increase the accuracy of process simulations at the expense of other OED efficiencies, e.g. D-efficiency for parameter accuracy. However, efficient trade-off solutions can be identified balancing process simulation and parameter accuracy. Balanced compound or multi-objective designs allow to identify such trade-off solutions.

Considering multiple operating points of the process simulation instead of only one operating point, e.g. by L- or D_k-optimality

[4,27], could extend the accuracy increase by c-OED for a broader simulation range of the process model. For an extension from process simulation to process optimisation and design, the sensitivities of the optimal process variables to the uncertain property parameters need to be considered. For example, the first-order derivatives of optimised process simulation outputs with respect to property parameters could be integrated into c-OED. Ultimately, this approach would formally transform the idea of c-OED into the method of weighted A-optimality presented by [21]. Moreover, in practice, the initial parameter guesses rarely match the optimal parameters. Thus, an iterative procedure is usually required [57] that involves not only OED but also parameter fitting, validation and consistency tests. Therefore, future work should investigate the influence of initial property parameters on the benefit from c-optimal design.

Declaration of Competing Interest

The authors declare that they have no known competing financial interests or personal relationships that could have appeared to influence the work reported in this paper.

CRediT authorship contribution statement

Lorenz Fleitmann: Conceptualization, Methodology, Validation, Software, Investigation, Data curation, Visualization, Writing – original draft, Writing – review & editing. **Jan Pyschik:** Methodology, Software, Investigation, Visualization, Writing – review & editing. **Ludger Wolff:** Conceptualization, Methodology, Software, Writing – review & editing. **Johannes Schilling:** Methodology, Validation, Investigation, Writing – review & editing. **André Bardow:** Conceptualization, Methodology, Writing – review & editing, Supervision, Funding acquisition.

Acknowledgments

The authors gratefully acknowledge funding by the Deutsche Forschungsgemeinschaft (DFG, German Research Foundation) under Germany's Excellence Strategy and Cluster of Excellence 2186 "The Fuel Science Center" ID: 390919832.

Supplementary material

Supplementary material associated with this article can be found, in the online version, at doi:10.1016/j.fluid.2022.113420.

References

[1] A. Mitsos, N. Asprion, C.A. Floudas, M. Bortz, M. Baldea, D. Bonvin, A. Caspari, P. Schäfer, Challenges in process optimization for new feedstocks and energy sources, Comput. Chem. Eng. 113 (2018) 209–221, doi:10.1016/j.compchemeng.2018.03.013.

[2] P.M. Mathias, Effect of VLE uncertainties on the design of separation sequences by distillation – Study of the benzene–chloroform–acetone system, Fluid Phase Equilib. 408 (2016) 265–272, doi:10.1016/j.fluid.2015.09.004.

[3] G.M. Kontogeorgis, R. Dohrn, I.G. Economou, J.-C. de Hemptinne, A. ten Kate, S. Kuitunen, M. Mooijer, L.F. Žilnik, V. Vesovic, Industrial requirements for thermodynamic and transport properties: 2020, Ind. Eng. Chem. Res. 60 (13) (2021) 4987–5013, doi:10.1021/acs.iecr.0c05356.

[4] A.C. Atkinson, A.N. Donev, R. Tobias, Optimum experimental designs, with SAS, Oxford statistical science series, vol. 34, Oxford University Press, Oxford and New York, 2006. http://search.ebscohost.com/login.aspx?direct=true&scope=site&db=nlebk&db=nlabk&AN=201173

[5] G. Franceschini, S. Macchietto, Model-based design of experiments for parameter precision: state of the art, Chem. Eng. Sci. 63 (19) (2008) 4846–4872, doi:10.1016/j.ces.2007.11.034.

[6] E. Forte, E. von Harbou, J. Burger, N. Asprion, M. Bortz, Optimal design of laboratory and pilot-plant experiments using multiobjective optimization, Chemie Ingenieur Technik 89 (5) (2017) 645–654, doi:10.1002/cite.201600104.

[7] O. Walz, H. Djelassi, A. Caspari, A. Mitsos, Bounded-error optimal experimental design via global solution of constrained min–max program, Comput. Chem. Eng. 111 (2018) 92–101, doi:10.1016/j.compchemeng.2017.12.016.

[8] D. Dechambre, L. Wolff, C. Pauls, A. Bardow, Optimal experimental design for the characterization of liquid–liquid equilibria, Ind. Eng. Chem. Res. 53 (50) (2014) 19620–19627, doi:10.1021/ie5035573.

[9] B.P. Duarte, A.C. Atkinson, J.F. Granjo, N.M. Oliveira, A model-based framework assisting the design of vapor-liquid equilibrium experimental plans, Comput. Chem. Eng. 145 (2021) 107168, doi:10.1016/j.compchemeng.2020.107168.

[10] L. Wolff, H.-J. Koß, A. Bardow, The optimal diffusion experiment, Chem. Eng. Sci. 152 (2016) 392–402, doi:10.1016/j.ces.2016.06.012.

[11] L. Pronzato, E. Walter, Experiment design for bounded-error models, Math. Comput. Simul. 32 (5–6) (1990) 571–584, doi:10.1016/0378-4754(90)90013-9.

[12] Q. Dong, R.D. Chirico, X. Yan, X. Hong, M. Frenkel, Uncertainty reporting for experimental thermodynamic properties †, J. Chem. Eng. Data 50 (2) (2005) 546–550, doi:10.1021/je049673d.

[13] M. Gevers, L. Ljung, Optimal experiment designs with respect to the intended model application, Automatica 22 (5) (1986) 543–554, doi:10.1016/0005-1098(86)90064-6.

[14] N. Asprion, R. Böttcher, J. Mairhofer, M. Yliruka, J. Höller, J. Schwientek, C. Vanaret, M. Bortz, Implementation and Application of Model-Based Design of Experiments in a Flowsheet Simulator, J. Chem. Eng. Data (2019), doi:10.1021/acs.jced.9b00494.

[15] O. Walz, H. Djelassi, A. Mitsos, Optimal experimental design for optimal process design: a trilevel optimization formulation, AIChE J. 110 (2019) 971, doi:10.1002/aic.16788.

[16] S. Recker, N. Kerimoglu, A. Harwardt, O. Tkacheva, W. Marquardt, On the integration of model identification and process optimization, in: 23rd European Symposium on Computer Aided Process Engineering, in: Computer Aided Chemical Engineering, vol. 32, Elsevier, 2013, pp. 1021–1026, doi:10.1016/B978-0-444-63234-0.50171-8.

[17] S. Lucia, R. Paulen, Robust nonlinear model predictive control with reduction of uncertainty via robust optimal experiment design, IFAC Proc. Vol. 47 (3) (2014) 1904–1909, doi:10.3182/20140824-6-ZA-1003.02332.

[18] S. Kaiser, S. Engell, Integrating superstructure optimization under uncertainty and optimal experimental design in early stage process development, in: 30th European Symposium on Computer Aided Process Engineering, in: Computer Aided Chemical Engineering, vol. 48, Elsevier, 2020, pp. 799–804, doi:10.1016/B978-0-12-823377-1.50134-8.

[19] S. Kaiser, T. Menzel, S. Engell, Focusing experiments in the early phase process design by process optimization and global sensitivity analysis, in: 31st European Symposium on Computer Aided Process Engineering, in: Computer Aided Chemical Engineering, vol. 50, Elsevier, 2021, pp. 899–904, doi:10.1016/B978-0-323-88506-5.50139-X.

[20] L. Fleitmann, J. Pyschik, L. Wolff, A. Bardow, Optimal physical property data for process simulations by optimal experimental design, in: 31st European Symposium on Computer Aided Process Engineering, in: Computer Aided Chemical Engineering, vol. 50, Elsevier, 2021, pp. 851–857, doi:10.1016/B978-0-323-88506-5.50133-9.

[21] B. Houska, D. Telen, F. Logist, M. Diehl, J.F. van Impe, An economic objective for the optimal experiment design of nonlinear dynamic processes, Automatica 51 (2015) 98–103, doi:10.1016/j.automatica.2014.10.100.

[22] D. Telen, B. Houska, F. Logist, J. van Impe, Multi-purpose economic optimal experiment design applied to model based optimal control, Comput. Chem. Eng. 94 (2016) 212–220, doi:10.1016/j.compchemeng.2016.07.004.

[23] D. Telen, B. Houska, M. Vallerio, F. Logist, J. van Impe, A study of integrated experiment design for NMPC applied to the droop model, Chem. Eng. Sci. 160 (2017) 370–383, doi:10.1016/j.ces.2016.10.046.

[24] V.V. Fedorov, S.L. Leonov, Optimal Design for Nonlinear Response Models, Chapman & Hall, first ed., Taylor & Francis, Boca Raton, 2014.

[25] T. Holland-Letz, On the combination of c- and D-optimal designs: General approaches and applications in dose-response studies, Biometrics 73 (1) (2017) 206–213, doi:10.1111/biom.12545.

[26] T. Holland-Letz, N. Gunkel, E. Amtmann, A. Kopp-Schneider, Parametric modeling and optimal experimental designs for estimating isobolograms for drug interactions in toxicology, J. Biopharma. Stat. 28 (4) (2018) 763–777, doi:10.1080/10543406.2017.1397005.

[27] T. Holland-Letz, A. Kopp-Schneider, Optimal experimental designs for estimating the drug combination index in toxicology, Comput. Stat. Data Anal. 117 (2018) 182–193, doi:10.1016/j.csda.2017.08.006.

[28] C. Han, K. Chaloner, D- and c-optimal designs for exponential regression models used in viral dynamics and other applications, J. Stat. Plann. Inference 115 (2) (2003) 585–601, doi:10.1016/S0378-3758(02)00175-1.

[29] Y. Bard, Nonlinear Parameter Estimation, Acad. Press, New York, 1974.

[30] H. Renon, J.M. Prausnitz, Local compositions in thermodynamic excess functions for liquid mixtures, AIChE J. 14 (1) (1968) 135–144, doi:10.1002/aic.690140124.

[31] A. Bazyleva, J. Abildskov, A. Anderko, O. Baudouin, Y. Chernyak, J.-C. de Hemptinne, V. Diky, R. Dohrn, J.E. Richard, J. Jacquemin, J.-N. Jaubert, K.G. Joback, U.R. Kattner, G. Kontogeorgis, H. Loria, P.M. Mathias, J.P. O'Connell, W. Schröer, G.J. Smith, A. Soto, S. Wang, R.D. Weir, Good reporting practice for thermophysical and thermochemical property measurements (IUPAC technical report), Pure Appl. Chem. Chimie pure et Appliquee 93 (2) (2021), doi:10.1515/pac-2020-0403.

[32] H.C. van Ness, Thermodynamics in the treatment of vapor/liquid equilibrium (VLE) data, Pure Appl. Chem. Chimie pure et Appliquee 67 (6) (1995) 859–872, doi:10.1351/pac199567060859.

[33] J. Gmehling, M. Kleiber, Vapor–liquid equilibrium and physical properties for distillation, in: Distillation, Elsevier, 2014, pp. 45–95, doi:10.1016/B978-0-12-386547-2.00002-8.

[34] W. Squire, G. Trapp, Using complex variables to estimate derivatives of real functions, SIAM Rev. 40 (1) (1998) 110–112, doi:10.1137/S003614459631241X.
[35] R. García-Ródenas, J.C. García-García, J. López-Fidalgo, J.Á. Martín-Baos, W.K. Wong, A comparison of general-purpose optimization algorithms for finding optimal approximate experimental designs, Comput. Stat. Data Anal. 144 (2020) 106844, doi:10.1016/j.csda.2019.106844.
[36] Y. Yu, Monotonic convergence of a general algorithm for computing optimal designs, Ann. Stat. 38 (3) (2010) 1593–1606, doi:10.1214/09-AOS761.
[37] H.P. Wynn, Results in the Theory and construction of D-optimum experimental designs, J. R. Stat. Soc. Ser. B 34 (2) (1972) 133–147, doi:10.1111/j.2517-6161.1972.tb00896.x.
[38] N.-K. Nguyen, A.J. Miller, A review of some exchange algorithms for constructing discrete D-optimal designs, Comput. Stat. Data Anal. 14 (4) (1992) 489–498, doi:10.1016/0167-9473(92)90064-M.
[39] J. Bausa, R.v. Watzdorf, W. Marquardt, Shortcut methods for nonideal multicomponent distillation: I. Simple columns, AIChE J. 44 (10) (1998) 2181–2198, doi:10.1002/aic.690441008.
[40] C. Redepenning, S. Recker, W. Marquardt, Pinch-based shortcut method for the conceptual design of isothermal extraction columns, AIChE J. 63 (4) (2017) 1236–1245, doi:10.1002/aic.15523.
[41] T.H. Chilton, A.P. Colburn, Distillation and absorption in packed columns a convenient design and correlation method, Ind. Eng. Chem. 27 (3) (1935) 255–260, doi:10.1021/ie50303a004.
[42] Thermal Separation Processes: Chapter 01 - Basic Concepts, K. Sattler, H.J. Feindt (Eds.), Wiley-VCH Verlag GmbH, Weinheim, Germany, 1995, doi:10.1002/9783527615476.
[43] S. Enders, H. Kahl, J. Winkelmann, Surface tension of the ternary system water + acetone + toluene, J. Chem. Eng. Data 52 (3) (2007) 1072–1079, doi:10.1021/je7000182.
[44] B. Kuzmanović, M.L. van Delden, N.J.M. Kuipers, A.B. de Haan, Fully automated workstation for liquid−liquid equilibrium measurements, J. Chem. Eng. Data 48 (5) (2003) 1237–1244, doi:10.1021/je0340452.
[45] D. Dechambre, C. Pauls, L. Greiner, K. Leonhard, A. Bardow, Towards automated characterisation of liquid–liquid equilibria, Fluid Phase Equilib. 362 (2014) 328–334, doi:10.1016/j.fluid.2013.10.048.
[46] J. Thien, L. Reinpold, T. Brands, H.-J. Koß, A. Bardow, Automated physical property measurements from calibration to data analysis: microfluidic platform for liquid–liquid equilibrium using raman microspectroscopy, J. Chem. Eng. Data 65 (2) (2020) 319–327, doi:10.1021/acs.jced.9b00636.
[47] E. Forte, A. Kulkarni, J. Burger, M. Bortz, K.-H. Küfer, H. Hasse, Multi-criteria optimization for parametrizing excess Gibbs energy models, Fluid Phase Equilib. 522 (2020) 112676, doi:10.1016/j.fluid.2020.112676.
[48] L.W.M. Wolff, From model-based experimental design and analysis of diffusion and liquid-liquid equilibria to process applications, RWTH Aachen University, Aachen, Germany, 2021 Ph.D. thesis.
[49] L.T. Biegler, I.E. Grossmann, A.W. Westerberg, Systematic methods of chemical process design, Prentice-Hall international series in the physical and chemical engineering sciences, Prentice-Hall, Upper Saddle River, NJ, 1997.
[50] I. Nagata, Liquid-liquid equilibria for four ternary systems containing methanol and cyclohexane, Fluid Phase Equilib. 18 (1) (1984) 83–92, doi:10.1016/0378-3812(84)80023-0.
[51] I. Nagata, Liquid-liquid equilibria for ternary acetonitrile-ethanol-saturated hydrocarbon and acetonitrile-1-propanol-saturated hydrocarbon mixtures, Thermochimica Acta 119 (2) (1987) 357–368, doi:10.1016/0040-6031(87)80272-1.
[52] J. Thien, C. Peters, T. Brands, H.-J. Koß, A. Bardow, Efficient determination of Liquid–Liquid equilibria using microfluidics and raman microspectroscopy, Ind. Eng. Chem. Res. 56 (46) (2017) 13905–13910, doi:10.1021/acs.iecr.7b03230.
[53] The MathWorks Inc., MATLAB: Optimization Toolbox (Release 2019a)., 2019.
[54] A. Mitsos, G.M. Bollas, P.I. Barton, Bilevel optimization formulation for parameter estimation in liquid–liquid phase equilibrium problems, Chem. Eng. Sci. 64 (3) (2009) 548–559, doi:10.1016/j.ces.2008.09.034.
[55] A.C. Atkinson, B. Bogacka, Compound and other optimum designs for systems of nonlinear differential equations arising in chemical kinetics, Chemom. Intell. Lab. Syst. 61 (1–2) (2002) 17–33, doi:10.1016/S0169-7439(01)00173-3.
[56] C.R. Rojas, J.S. Welsh, G.C. Goodwin, A. Feuer, Robust optimal experiment design for system identification, Automatica 43 (6) (2007) 993–1008, doi:10.1016/j.automatica.2006.12.013.
[57] A.R.G. Mukkula, M. Mateáš, M. Fikar, R. Paulen, Robust multi-stage model-based design of optimal experiments for nonlinear estimation, Comput. Chem. Eng. (2021) 107499, doi:10.1016/j.compchemeng.2021.107499.